Full . Published Online: June 2017 Accepted: May 2017

Use of micro-photoluminescence as a contactless measure of the 2D electron density in a GaAs quantum well

Appl. Phys. Lett. **110**, 262104 (2017); https://doi.org/10.1063/1.4985439

D. Kamburov[1], K. W. Baldwin[1], K. W. West[1], S. Lyon[1], L. N. Pfeiffer[1], *and* A. Pinczuk[2]

KEYWORDS

Quantum wells
Photoluminescence
Carrier density
Electric measurements
Density measurement

ABSTRACT

We compare micro-photoluminescence (μPL) as a measure of the electron density in a clean, two-dimensional (2D) system confined in a GaAs quantum well (QW) to the standard magneto-transport technique. Our study explores the PL shape evolution across a number of molecular beam epitaxy-grown samples with different QW widths and 2D electron densities and notes its correspondence with the density obtained in magneto-transport measurements on these samples. We also measure the 2D density in a top-gated quantum well sample using both PL and transport and find that the two techniques agree to within a few percent over a wide range of gate voltages. We find that the PL measurements are sensitive to gate-induced 2D density changes on the order of 10^9 electrons/cm^2. The spatial resolution of the PL density measurement in our experiments is 40 μm, which is already

substantially better than the millimeter-scale resolution now possible in spatial density mapping using magneto-transport. Our results establish that μPL can be used as a reliable high spatial resolution technique for future contactless measurements of density variations in a 2D electron system.

Engineered two-dimensional electron systems (2DESs) provide a fertile ground for studying fundamental physical phenomena, including the integer quantum Hall effect (IQHE) and the fractional quantum Hall effect (FQHE).[1,2] Advances in molecular beam epitaxy (MBE) technology[3] allow the precise control of growth parameters, which critically affect scattering mechanisms and carrier mobilities,[4–8] and offer high material quality, with long carrier mean-free paths and high mobilities.[9] The progress in MBE-grown samples has been verified by numerous detailed transport measurements.[10] Thus far, however, optical techniques have had little overlap with transport techniques.[11–25] More specifically, there are no systematic studies of the photoluminescence (PL) spectra from different GaAs structures or for their use in determining the 2DES density. The lack of systematic reports at the intersection of optical and transport measurements is surprising given the important role PL could play in understanding subtle material properties. In particular, a study of local density variations in GaAs samples could be used to track sources of impurities in the conducting channel and to measure local differences in the dopant efficiency. Here, we focus on the comparison between transport and optical measurements with the goal of

establishing micro-photoluminescence (μPL) as a viable technique for characterizing the carrier concentration in GaAs quantum wells (QWs) and for investigating possible small local density variations in these 2D systems.

We begin by exploring the PL spectra of a set of 2DESs confined to single-sided delta-doped, MBE-grown GaAs QWs of various QW widths on (001) GaAs substrates. We compare the carrier densities measured by μPL to transport measurements. The samples in our study are each modulation-doped with Si to nominal electron densities in the range of $n \simeq 2.0$ to 4.0×10^{11} cm^{-2}. The 2D electrons in these samples are located 260 nm under the surface and are flanked on each side by undoped $Al_{0.32}Ga_{0.68}As$ setback layers. The QW widths range from $W = 10$–26 nm. These structures are engineered so that the second sub-band is at least 10 meV above the Fermi energy so that we can avoid Fermi edge singularity issues. Transport measurements on each sample were conducted in a van der Pauw configuration with annealed InSn contacts in a ^{3}He refrigerator with a base temperature of $T \simeq 0.3$ K using standard low-frequency lock-in amplifier techniques. The PL density values were determined using 1.2 μW of power focused on a 40 μm diameter spot from a 730 nm laser in a continuous-flow cryostat with the samples at a temperature of 7.2 K. The laser focus spot size was chosen for convenience to provide a sufficiently low power density of 75 mW/cm^2 with reasonably fast data acquisition times. Samples in PL measurements

always had at least one annealed InSn Ohmic contact. For the gating part of the experiment, the carrier density in the 21.2 nm QW sample was changed using a 4 nm thick transparent front gate of Titanium (Ti) metal.

The main features of the PL spectrum and their relation with the 2DEG carrier density are summarized in Fig. 1. The laser light creates electron-hole pairs which in turn induce recombinations between the 2D electron states in the QW, residing in the lowest $n = 1$ energy level of the conduction band, and hole states created by the laser absorption in the valence band. These recombinations preserve momentum and appear as vertical transitions on the momentum (k) diagram. The QW PL spectrum has a characteristic shape with a strong maximum near the bottom of the QW band, at E_0, and a Fermi-like shape at $E_0 + \Delta E$. Both points can easily be determined from the derivative of the PL spectrum: E_0 is a zero of the derivative, while $E_0 + \Delta E$ is a local maximum. Taking into account the Burstein-Moss shift,[26,27] the Fermi energy is $E_F = \Delta E/(1 + m_e^*/m_h^*)$, where ΔE is the energy difference between the PL spectral peak at E_0 corresponding to the bottom of the band, and the high energy edge of the PL spectral wing related to maximal Fermi filling, and m_e^* and m_h^* are the effective electron and hole masses, respectively.[14,23] Since for a 2D system $n = g_{2D}E_F$, where $g_{2D} = 2.8\times 10^{10}\,\mathrm{meV^{-1}\,cm^{-2}}$ is the 2D electron density of states for GaAs,[28] this relation provides a direct measurement of the 2DEG carrier density from the PL spectrum. It is insensitive to first order to band gap

renormalization effects. We emphasize that the analysis of the PL spectrum is not unique to single-sided QWs and that similar PL spectra were obtained from QWs doped from both sides.

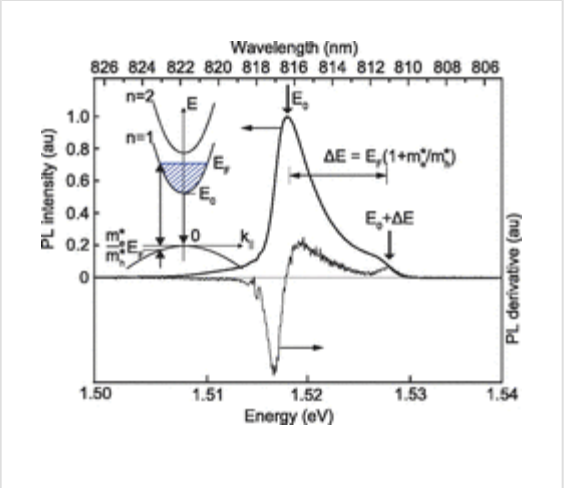

FIG. 1.

Normalized μPL spectrum and its derivative as a function of energy in a 21.2 nm GaAs QW. The spectrum shows a pronounced peak E_0 at the bottom of the QW energy band and a Fermi edge at $E_0 + \Delta E$. Both energy points are well defined on the derivative traces as a zero and a local maximum, respectively. Inset: Schematic of the optical processes which define the PL line shape. The density of carriers in the QW can be measured directly from the μPL spectrum, taking into account the curvature of the band and approximating it as parabolic with effective masses m_e^* and m_h^* (see text).

PPT | High-resolution

In Fig. 2, we plot the temperature dependence of the PL spectra for the 21.2 nm wide QW. The E_0 peak position remains

unchanged as the temperature increases from 7.2 K to 27.4 K although the peak broadens. The Fermi edge also remains at the same energy, but the shoulder step height lifts up at higher temperatures because the photo-induced holes have more kinetic energy and thus populate more high-momentum states. Similar temperature behavior is observed for all QW widths and 2D densities. The increase of the shoulder intensity at $E_0 + \Delta E$ relative to the peak at E_0 with temperature has been shown as a signature of the Fermi edge.[14,20–22,24] Although at high temperatures the Fermi edge is very pronounced, lower-temperature traces, with $8 < T < 11.3$ K, are generally more useful for high precision measurements of the carrier density because the Fermi edge is better defined, and the uncertainty in the derivative peak at $E_0 + \Delta E$ is the smallest.

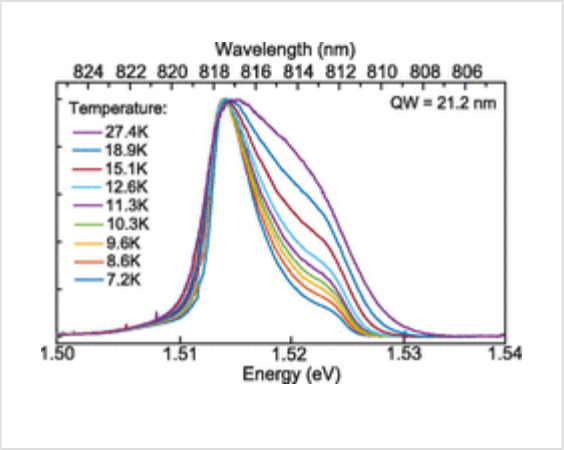

FIG. 2.

Photoluminescence spectra of the 21.2 nm QW as a function of energy at different sample temperatures. All traces are normalized to the maximum value of the E_0 peak.

PPT | High-resolution

Figure 3(a) shows PL traces as a function of density for three structures with a 21.2 nm wide QW measured at 7.2 K. The arrows indicate the measured positions of the E_0 and E_F points. As the electron density increases, the Fermi edge shoulder extends to higher energies since more states in the QW are occupied. The E_0 peak moves to lower energies as the bandgap decreases with higher electron density.[29] In several of these μPL spectra, a pronounced peak emerges near 818 nm, which is attributed to the free exciton peak in high quality GaAs.[30]

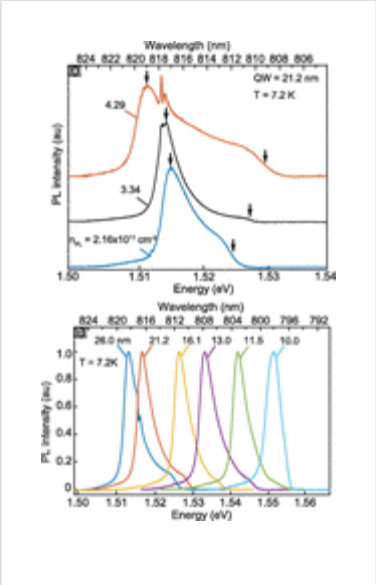

FIG. 3.

Photoluminescence spectra as functions of energy and wavelength for samples with different electron densities (a) and QWs (b) at $T = 7.2$ K.

PPT | High-resolution

The dependence of the μPL spectra on the QW width is summarized in Fig. 3(b) for 6 samples of nominal 2D density $n \simeq 3 \times 10^{11}$ cm^{-2} with various QW widths measured at 7.2 K. When the QW width is large, the traces exhibit a strong peak at

E_0 and a pronounced shoulder near the Fermi edge.[30–32] As the QW width gets narrower, the height of the Fermi step gradually becomes less pronounced, degrading at 11.5 nm and eventually disappearing in the 10 nm QW spectrum. A zero height Fermi edge step makes it impossible to see the location of the Fermi edge, which causes the PL spectrum to resemble that of an empty QW. We speculate that this behavior might be due to the fact that the 2D holes produced by photon absorption get trapped near zero momentum in QW width fluctuations at the narrower QWs. The corresponding densities of the samples, measured with PL and transport, are summarized in Table I. Except for the narrowest QWs, the PL and transport densities agree to within 12%.

TABLE I. 2DEG density measured with transport (n_{tr}) and PL (n_{PL}).

In order to provide a more comprehensive understanding of the behavior of the PL spectra as a function of carrier density, we varied the bias $V_{\mathbf{fg}}$ of a thin Ti gate on the top surface of a 21.2 nm QW sample. The front gate is thin enough to allow the laser light and the PL to pass through. Figure 4(a) shows the PL spectra vs $V_{\mathbf{fg}}$. At very high (>0.3 V) and very low (<–0.7 V) gate voltages, the PL shape does not change significantly. In the middle of the front-gate voltage range, the spectra change gradually: for positive bias, they appear very similar to the

unbiased spectrum shown in Fig. 3(b), while as the bias becomes negative, the E_0 peak moves closer to the Fermi edge. In all cases, the Fermi edge remains at the same energy but, as the carrier density gets very low, it starts to look like the spectrum of an empty QW. Note that placing the Ti gate on the top surface of the sample reduces the carrier density measured with PL from 3.21 to 2.49×10^{11} cm^{-2}. This shift is real and is confirmed in the transport measurements.

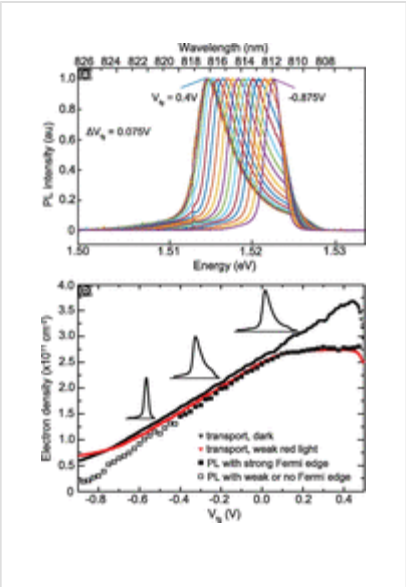

FIG. 4.

(a) Photoluminescence spectra of the 21.2 nm sample as a function of energy at different front gate voltages. The voltages vary in equal steps of $\Delta V = 0.075$ V from $V_{fg} = 0.4$V to –0.875 V. All traces are normalized to the value of the E_0 peak. (b) Comparison between the transport and PL densities measured on the same 21.2 nm QW as a function of front gate voltage. The transport density is represented by black and red triangles in the dark at 300 mK and with light at 4 K, respectively. The PL data are shown with squares. Filled squares represent PL traces with clear Fermi edge while the open squares correspond to data from PL traces with weak or absent Fermi edge.

The 2D densities measured by transport and PL techniques are compared as a function of front-gate voltage in Fig. 4(b). The figure shows PL data alongside the results from transport measurements from the 21.2 nm sample at 0.3 K in the dark and at 4 K with a red diode on. We emphasize several interesting points: (i) there is a range of front-gate voltages, between $V_{\mathbf{fg}} = -0.4$ V and 0.1 V, for which the three methods give the same density to within 5%; (ii) for $V_{\mathbf{fg}} < -0.4$ V the PL traces lack a pronounced Fermi edge so that the density measured with PL significantly deviates from the transport densities; (iii) for $V_{\mathbf{fg}} < 0.4$V, the PL and the transport measurements with the light on agree well, while the transport measurements in the dark deviate significantly; (iv) leakage of the front-gate for voltages $V_{\mathbf{fg}} > 0.4$V can be seen in all three measurement methods; (v) when the weak red light is on, excessive carrier creation makes the front gate ineffective in changing the carrier density at positive bias. We note that condition (i) defines a working range of carrier densities $n > 1.5 \times 10^{11}$ cm^{-2} above which the μPL technique is found to be reliable. Overall, the PL and the transport measurement agree very well for a large range of front-gate voltages across which the carrier density changes by a factor of 2. We find the PL measurement to be sensitive to carrier density variations as

small as 10 cm .

To summarize, our data reveal that the PL spectra exhibit a strong peak near the bottom of the QW, at E_0, and a pronounced Fermi edge in a number of QWs. The carrier density can be changed with a thin transparent front-gate, and both transport and PL measurements agree very well for a range of front-gate voltages over which the carrier density changes by a factor of 2. The agreement defines a range of densities $n > 1.5 \times 10^{11}$ cm^{-2} above which the μPL technique is reliable, provided we maintain a separation of 5–10 meV between the Fermi level and the second sub-band of the quantum well. The PL measurements are very sensitive to gate-induced density variations and can detect changes as small as 10^9 cm^{-2}. Coupled with the small size of the laser beam, our results affirm PL as a viable technique for detecting small and spatially local density variations. Since transport measurements are carried on bulk samples, often several millimeters in size, the μPL technique provides a significant improvement in characterizing GaAs samples locally and paves the way for future experiments that use photoluminescence to probe the sample quality of these 2D systems.

We acknowledge support through the Gordon and Betty Moore Foundation (Grant No. GBMF4420) and NSF (DMR-1305691, ECCS-1508925, MRSEC DMR-1420541). The work at Columbia was supported by the U.S. National Science Foundation Division of Materials Research (Award No. DMR-

1306976) and by the U.S. Department of Energy Office of Science, Division of Materials Science and Engineering (Award No. DE-SC0010695).

REFERENCES

1.

K. von Klitzing , G. Dorda , and M. Pepper , Phys. Rev. Lett. **45**, 494–497 (1980). https://doi.org/10.1103/PhysRevLett.45.494, **Google Scholar**, **Crossref**, **CAS** Open URL

2.

D. C. Tsui , H. L. Stormer , and A. C. Gossard , Phys. Rev. Lett. **48**, 1559 (1982). https://doi.org/10.1103/PhysRevLett.48.1559, **Google Scholar**, **Crossref**, **CAS** Open URL

3.

A. Y. Cho , J. Appl. Phys. **41**, 2780 (1970). https://doi.org/10.1063/1.1659315, **Google Scholar**, **Scitation**, **CAS** Open URL

4.

M. Santos , T. Sajoto , A. Zrenner , and M. Shayegan , Appl. Phys. Lett. **53**, 2504 (1988). https://doi.org/10.1063/1.100225,

Google Scholar, **Scitation**, **CAS** Open URL

5.

T. Sajoto , M. Santos , J. J. Heremans , M. Shayegan , M. Heiblum , M. V. Weckwerth , and U. Meirav , Appl. Phys. Lett. **54**, 840 (1989). https://doi.org/10.1063/1.100862, **Google Scholar**, **Scitation**, **CAS** Open URL

6.

M. Shayegan , V. J. Goldman , M. Santos , T. Sajoto , L. Engel , and D. C. Tsui , Appl. Phys. Lett. **53**, 2080 (1988). https://doi.org/10.1063/1.100306, **Google Scholar**, **Scitation**, **CAS** Open URL

7.

R. Kohrbruck , S. Munnix , D. Bimberg , D. E. Mars , and J. N. Miller , Appl. Phys. Lett. **57**, 1025 (1990). https://doi.org/10.1063/1.103554, **Google Scholar**, **Scitation** Open URL

8.

W. T. Masselink , Y. L. Sun , R. Fischer , T. J. Drummond , Y. C. Chang , M. V. Klein , and H. Morkoc , J. Vac. Sci. Technol., B **2**, 117 (1984). https://doi.org/10.1116/1.582929, **Google Scholar**, **Crossref**, **CAS** Open URL

9.

L. N. Pfeiffer , K. W. West , H. L. Stormer , and K. W. Baldwin , Appl. Phys. Lett. **55**, 1888 (1989). https://doi.org/10.1063/1.102162, **Google Scholar**, **Scitation**, **CAS** Open URL

10.

M. Shayegan , " Flatland Electrons in High Magnetic Fields," in *High Magnetic Fields: Science and Technology, Theory and Experiment*, edited by F. Herlach and N. Miura (World Scientific, Singapore, 2006), Vol. 3, pp. 31–60 (2006). **Google Scholar**, **Crossref** Open URL

11.

D. Olego and M. Cardona , Phys. Rev. B **22**, 886 (1980). https://doi.org/10.1103/PhysRevB.22.886, **Google Scholar**, **Crossref**, **CAS** Open URL

12.

A. Pinczuk and J. M. Worlock , Surf. Sci. **113**, 69 (1982). https://doi.org/10.1016/0039-6028(82)90564-7, **Google Scholar**, **Crossref**, **CAS** Open URL

13.

J. Y. Marzin and E. V. K. Rao , Appl. Phys. Lett. **43**, 560 (1983). https://doi.org/10.1063/1.94419, **Google Scholar**,

Scitation, **CAS** Open URL

14.

A. Pinczuk , J. Shah , R. C. Miller , A. C. Gossard , and W. Wiegmann , Solid State Commun. **50**, 735 (1984). https://doi.org/10.1016/0038-1098(84)90975-X,
Google Scholar, **Crossref**, **CAS** Open URL

15.

F. Meseguer , J. C. Maan , and K. Ploog , Phys. Rev. B **35**, 2505 (1987). https://doi.org/10.1103/PhysRevB.35.2505,
Google Scholar, **Crossref**, **CAS** Open URL

16.

M. S. Skolnick , J. M. Rorison , K. J. Nash , and S. J. Bass , Surf. Sci. **196**, 507–511 (1988). https://doi.org/10.1016/0039-6028(88)90733-9,
Google Scholar, **Crossref**, **CAS** Open URL

17.

P. B. Kirby , J. A. Constable , and R. S. Smith , Phys. Rev. B **40**, 3013 (1989). https://doi.org/10.1103/PhysRevB.40.3013,
Google Scholar, **Crossref**, **CAS** Open URL

18.

R. Cingolani , W. Stolz , Y. H. Zhang , and K. Ploog , J.

Lumin. **46**, 147–154 (1990). https://doi.org/10.1016/0022-2313(90)90015-4, **Google Scholar**, **Crossref**, **CAS** Open URL

19.

Y. H. Zhang , N. N. Ledentsov , and K. Ploog , Phys. Rev. B **44**, 1399(R) (1991). https://doi.org/10.1103/PhysRevB.44.1399 , **Google Scholar**, **Crossref** Open URL

20.

Y. H. Zhang and K. Ploog , Phys. Rev. B **45**, 14069 (1992). https://doi.org/10.1103/PhysRevB.45.14069, **Google Scholar**, **Crossref**, **CAS** Open URL

21.

Y. F. Chen , L. Y. Lin , J. L. Shen , and D. W. Liu , Phys. Rev. B **46**, 12433 (1992). https://doi.org/10.1103/PhysRevB.46.12433, **Google Scholar**, **Crossref**, **CAS** Open URL

22.

P. A. Folkes , M. Dutta , S. Rudin , H. Shen , W. Zhou , D. D. Smith , M. Taysing-Lara , P. Newman , and M. Cole , Phys. Rev. Lett. **71**, 3379 (1993). https://doi.org/10.1103/PhysRevLett.71.3379, **Google Scholar** , **Crossref**, **CAS** Open URL

23.

F. Plentz , F. Meseguer , J. Sanchez-Dehesa , N. Mestres , and E. A. Meneses , Phys. Rev. B **48**, 1967 (1993). https://doi.org/10.1103/PhysRevB.48.1967, **Google Scholar**, **Crossref**, **CAS** Open URL

24.

T. A. Fisher , P. E. Simmonds , M. S. Skolnick , A. D. Martin , and R. S. Smith , Phys. Rev. B **48**, 14253 (1993). https://doi.org/10.1103/PhysRevB.48.14253, **Google Scholar**, **Crossref**, **CAS** Open URL

25.

S. J. Xu , S. J. Chua , X. H. Tang , and X. H. Zhang , Phys. Rev. B **54**, 17701 (1996) https://doi.org/10.1103/PhysRevB.54.17701. **Google Scholar**, **Crossref**, **CAS** Open URL

26.

E. Burstein , Phys, Rev. **93**, 632 (1954). https://doi.org/10.1103/PhysRev.93.632, **Google Scholar**, **Crossref**, **CAS** Open URL

27.

T. S. Moss , Proc. Phys. Soc. B **76**, 775 (1954). https://doi.org/10.1088/0370-1301/67/10/306, **Google Scholar**

, **Crossref** Open URL

28.

J. Davies , *The Physics of Low-Dimensional Systems* (Cambridge University Press, 1998), Fig. 1.9(b), p. 27. **Google Scholar**, Open URL

29.

S. C. Jain and D. J. Roulston , Solid-State Electron. **34**, 453 (1991). https://doi.org/10.1016/0038-1101(91)90149-S, **Google Scholar**, **Crossref**, **CAS** Open URL

30.

K. Kudo , Y. Makita , I. Takayasu , and T. Nomura , J. Appl. Phys. **59**, 888 (1986). https://doi.org/10.1063/1.336559, **Google Scholar**, **Scitation**, **CAS** Open URL

31.

J. Pastrnak , J. Oswald , M. Laznicka , A. Bosacchi , and A. Salokatva , Phys. Status Solidi **118**, 567 (1990). https://doi.org/10.1002/pssa.2211180230, **Google Scholar**, **Crossref**, **CAS** Open URL

32.

F. Schläpfer , W. Dietsche , C. Reichl , S. Faelt , and W. Wegscheider , J. Cryst. Growth **442**, 114–120 (2016).

https://doi.org/10.1016/j.jcrysgro.2016.02.039,